

SIMPLIFIED DESIGN APPROACH OF STEEL FIBER REINFORCED CONCRETE UNDER FLEXURAL FATIGUE LOAD

M. ADEL^{*}, K. NAGAI[†], AND K. MATSUMOTO^{††}

^{*}, [†] Institute of Industrial Science
The University of Tokyo, Tokyo, Japan
e-mail: adel@iis.u-tokyo.ac.jp
e-mail: nagai325@iis.u-tokyo.ac.jp

^{††} Division of Engineering and Policy for Sustainable Environment
Faculty of Engineering
Hokkaido University, Sapporo, Japan
e-mail: km312@eng.hokudai.ac.jp

Keywords: Steel Fiber Reinforced Concrete, Tension Softening Curve, Flexural Fatigue Loading, Fatigue Life, Section Analysis Calculation

Abstract: Several concrete structures such as bridges are often under fatigue loads. These loads lead to stiffness degradation of these structural members and result in damages at the micro level that finally cause a fatigue failure. Even though steel fibers have a great influence in improving the structural response of reinforced concrete (RC) members under different loading conditions, recent experimental tests at the material level indicated that the steel fibers improve resistance to crack growth, decrease deflection, and increase the fatigue life compared to the plain concrete under fatigue loading. Some concerns recently arose on the possibilities of enhancing the fatigue performance at the structural level using steel fiber reinforced concrete (SFRC), compared to using conventional RC. This paper focuses on the experimental results of SFRC beams co-reinforced with conventional deformed rebars on a structural level under flexural static and fatigue test, and fiber reinforced concrete (FRC) beams on the material level tested under flexural static test. The flexural static and fatigue behavior of SFRC beams is investigated regarding to experimental results of tensile strain developed in rebars, concrete strain, and neutral axis position during loading. Considering a degradation of bridging strength - induced in the steel fibers by arresting cracks opening and obtained from the flexural static test of FRC beams - in section analysis calculation, the fatigue flexural behavior of SFRC beams can be evaluated successfully during fatigue life under different fatigue stress level.

1 INTRODUCTION

Extensive studies have been performed to understand the fatigue performance of plain concrete and RC, on both material and structural level [CEB, 1988 and Mallet, 1991], these studies show loss of stiffness, increasing of deflection, growth in crack length and width, and increasing permanent strain of

concrete under fatigue. Even though a complete understanding of the influence of the fatigue process on the response of RC structures is not accomplished yet.

Fatigue of concrete is a process of progressive changes in the material that may lead to micro-crack initiation and propagation developing macrocracks formation that grow

until failure happen [CEB, 1988], when the strain energy released overcomes the remaining cohesive strength in the concrete. In the case of RC, fatigue loads cause micro-cracking that affect stress concentration around the bar deformation, followed by crack propagation, and finally leading to fracture of the reinforcing bar [Mallet, 1991].

SFRC is a composite material reinforced with discrete, uniformly distributed randomly oriented fibers. By adding fibers, mechanical properties such as ductility, durability, energy absorption, fatigue, and toughness could be improved [Tejchman and Kozicki, 2010].

A wide range of experiments has been carried out with SFRC at the material level to evaluate the enhancement in fatigue performance [Lee and Barr, 2004]. In addition, a few researches studied the performance of SFRC at the structural level under fatigue loading [Parvez, 2015], that concluded a reduction of average tensile stresses in the conventional reinforcement compared with the RC specimens. However, numerous experiments are still needed to investigate the fatigue behavior of SFRC structural members and provide a design approach for SFRC structural members under fatigue load.

The standard design guidelines of RC structures typically involve a few material parameters describing the mechanical behavior of concrete, typically only compressive strength and Young's modulus. Furthermore, no design formulae contain the fracture toughness of concrete explicitly. Recently, much focus has been put on using the fracture mechanical properties in testing and design of SFRC [RILEM-TDF-162], based on the fact that fibers in RC have a toughness and fracture energy added to the mechanical properties of concrete. The basic fracture mechanical concept proposed to be applied in SFRC design is the stress (σ)-crack opening (ω) relationship, that is associated with the so-called curve (T-S-C). The T-S-C can describe the post-cracking behavior and express the resistance of concrete against crack development.

To understand the response of steel fibers in the structural member under fatigue loading

comprehensively, and to propose a simplified design procedure of SFRC, SFRC specimens are needed to be tested experimentally. Two series of specimens with 1.5% fiber volume are investigated comprising: one series of small notched-beams in the material level under 3-point loading test to investigate the T-S-C under static test following [JCI, 2003], and another series of large scale beams in the structural level under 4-point loading static and fatigue test using linear variable differential transformer (LVDT) and electronic strain gauges to monitor the deflection, rebar strain, concrete strain, and the neutral axis (N.A.) position.

2 OBJECTIVES

The main objective of this experimental work was a full understanding of the static and fatigue behavior of SFRC beams co-reinforced with conventional rebars by:

- (a) Measuring the evolution of the rebar strain, concrete strain, and N.A. position during static loading, and fatigue life under different fatigue stress level.
- (b) Fitting the experimental results with the results determined by an analytical cross-sectional model that is being an extension of the commonly used bending design model for RC under the max load level during fatigue life, assuming that the degradation in the bridging strength carried by fibers, and not considering any stiffness degradation for SFRC beams during fatigue life.

3 EXPERIMENTAL PROCEDURE

3.1 Materials and Mix Proportions

The materials that used in this study were Ordinary Portland Cement (OPC), coarse aggregates with max aggregate size 13.0-mm to improve the fresh property of concrete, fine aggregates, and high-performance air-entraining (AE) water reducing agent, in order to achieve the desired compressive strength 35-MPa of cylinder specimen with a diameter

Table 1: Mixture proportion for concrete

W/C	Unit weight (kg/m ³)					
	W	C	S	G	S.F.	SP
0.55	185	336	1055	706	117.8	5.05

W = water, C = cement, S = fine aggregate,
G = coarse aggregate, S.F. = steel fiber,
SP = high-performance air-entraining (AE)
water-reducing agent

Table 2: Properties of steel fibers

Shape of ends	L (mm)	Φ (mm)	Density (kg/m ³)	Tensile strength (MPa)	L/d
Hooked	35	0.55	7850	1050	65

L = length, Φ = diameter, L/ Φ = Aspect ratio

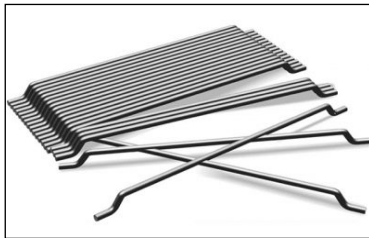


Figure 1: Hooked steel fibers.

100-mm and length 200-mm, and slump value of the fresh concrete on average 12-mm. Table 1 shows the mixture proportion of SFRC. Hooked end steel fibers are also added with 1.5% volume fraction of the full volume of the concrete. Figure 1 shows the geometry of the hooked steel fibers used in the test, and their properties are summarized in table 2.

diameter and 357-MPa yield strength.

3.2 Specimens

The experimental program consisted of two series. The first series consisted of six fiber reinforced concrete notched beams - material scale size - with a dimension of 100 x 100 x 400-mm, having a notch with dimensions of 100 x 30 x 5-mm at a mid-length of each specimen following the standard of Japan Concrete Institute [JCI, 2003]. The second series consisted of four SFRC beams - structural scale size - with a dimension of 150 x 200 x 2000-mm with an effective depth (d) of 170-mm and a length of the constant moment region of 300-mm, also were reinforced with two conventional rebars with a nominal diameter (D) of 16-mm. The test program is outlined in Table 3.

3.3 Testing Setup and Instrumentation

The beams were simply supported with span (L) of 300-mm for series one and 1700-mm for series two. The first series was tested under a three-point loading, as shown in Figure 2, and the second series was tested under a four-point loading test, as shown in Figure 3, all dimension in mm. Steel plates were placed on the pin-hinge supports and loading points.

The specimens were instrumented to

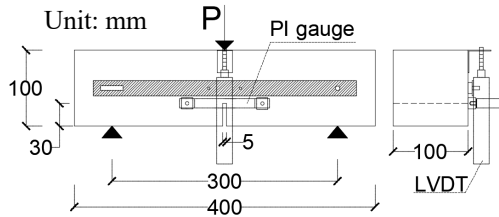
Table 3: Specimens data

Beam size level	Specimen ID	Test type	Span L (mm)	Constant moment region (mm)	Tensile rebars	Fiber volume (%)	Concrete properties			Load range (kN)	Fatigue life
							E _c GPa	f _c MPa	f _t MPa		
material	SNB-1	static	300	zero	-	1.5	25	35	3.4	-	-
	SNB-2										
	SNB-3										
	SNB-4										
	SNB-5										
	SNB-6										
structural	SLB-1	static	1700	300	2D16					-	-
	FLB-30	fatigue								5~30	2000000
	FLB-40									5~40	2000000
	FLB-50									5~50	380116

The longitudinal reinforcing rebars were made of deformed steel having 16.0-mm in nominal



(a) Real test setting for FRC beams.



(b) The geometry of FRC beams.

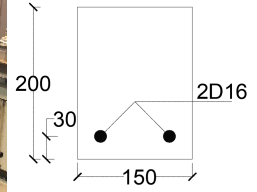
Figure 2: Detailed settings of FRC notched beams.

measure the steel strains, concrete strains, crack widths, and deflections. The deflections of mid-span and supporting points were measured using three LVDTs, and steel strains were measured using six 2-mm electrical resistance strain gauges attached to the rebars prior to concrete casting at the constant moment region. For measuring of the concrete strains, 60-mm electronic strain gauges were fixed at constant moment region in three stations with spacing 100-mm and at three levels from the top of beams with spacing 10-mm. crack width was measured using pi-gauges with 100-mm length attached at the tip of the notch.

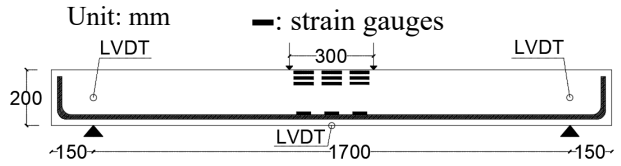
The load was applied through a 300-kN capacity loading actuator. For series one, the static load was applied under deflection control at 0.06-mm/min up to the peak load, then at a rate of 0.6-mm/min to completion. For series two, the static load was applied under deflection control at 0.6-mm/min up to the peak load, then at a rate of 1.8-mm/min to completion. In addition, for fatigue tests, the load was applied under deflection control at a rate 0.6-mm/min monotonically up to the median load of the load ranges, after that the fatigue load was applied using a sinusoidal wave under load control at frequency 5.0-Hz. The actuator was programmed to pause at



(a) Real test setting.



(b) Beam's x-section.



(c) Beam's Geometry.

Figure 3: Detailed settings of SFRC beams.

a certain interval during the fatigue loading to enable data recording and observation. Testing was undertaken continuously 24-hr a day until either failure or completion of two million cycles.

4 SECTION ANALYSIS CALCULATION

The flexure theory of traditional RC structures was used in the analysis of the SFRC beams that subjected to a pure bending in order to calculate the moment capacity of these beams.

Using the same assumptions of RC beams which are:

- (a) The plane section before bending remain plane after bending, which means that strain distribution is assumed to be linear following the beam theory.
- (b) Same strain in the rebars and concrete located at the same level, assuming perfect bond between concrete and rebars.
- (c) The stresses in the concrete and rebars can be calculated using the idealized stress-strain curves for concrete and steel.

Using the T-S-C representing the post-cracking tensile strength of FRC following [JCI, 2003] with the cracking tensile strength from the splitting tensile test could

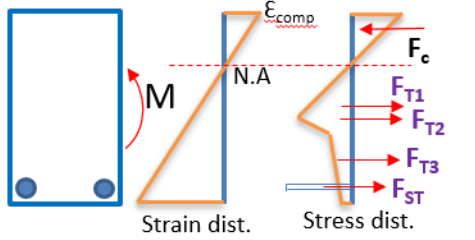


Figure 4: Stress and strain distribution of SFRC beam section.

$$\Sigma F_{internal} = \Sigma F_{external} \quad (1)$$

$$\Sigma M_{internal} = M_{external} \quad (2)$$

represent the tensile properties of FRC during the bending test.

The analysis was carried out by assuming a certain level of degradation of T-S-C during fatigue life, concrete strain, and N.A. position by satisfying equilibrium conditions in internal and external forces and moments, as shown in Figure 4 and equations 1 and 2. Finally, the rebar strain, concrete strain, and N.A. position that are resulted from the section analysis calculation are compared with the experimental value.

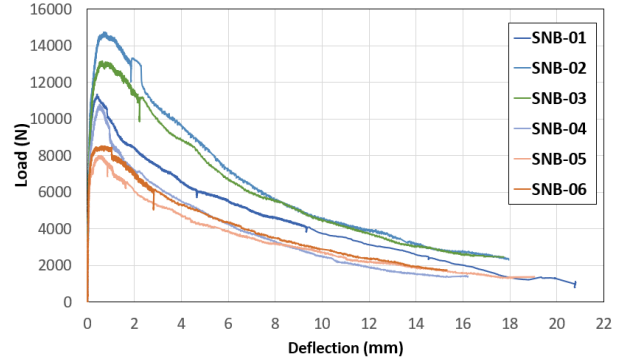
5 RESULTS AND DISCUSSION

5.1 Tension Softening Curve

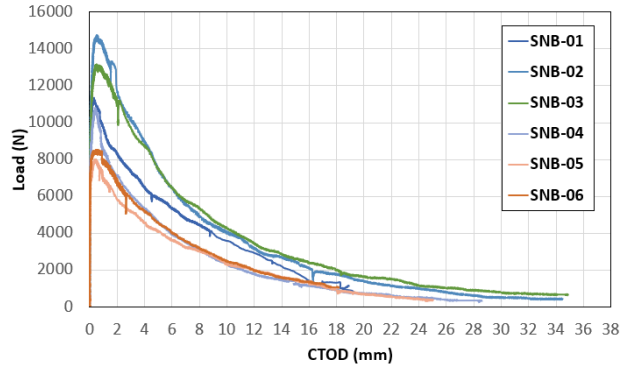
The T-S-C is one of the fracture mechanics parameters that can describe the post-cracking behavior and reflect the fracture energy (G_F). Instead of the direct tensile test, the T-S-C has been determined by the poly-linear approximation analysis method from the bending test of notched beams [JCI, 2003].

A static three-point loading flexure test was carried out for series one with monitoring load, deflection, and crack tip opening displacement. The results of six FRC notched beams were 11.1-kN as an average static flexural capacity with standard deviation 2.38-kN and 12.94-N/mm as an average fracture energy (G_F) with standard deviation 3.71-N/mm, as shown in Figure 5.

The T-S-C was investigated from the average load-load point displacement curve and load-crack tip opening displacement curve of six notched FRC beams of series one. Finally, the



(a) Load-load point deflection curve.



(b) Load-crack tip opening displacement curve.

Figure 5: Mechanical properties of FRC notched beams.

$$\begin{aligned} \sigma &= 3.4 \quad (\text{MPa}) \quad \text{for } \omega \leq 0.42 \text{ mm} \\ \sigma &= 3.7 - 0.72\omega \quad (\text{MPa}) \quad \text{for } \omega > 0.42 \text{ mm} \end{aligned} \quad (3)$$

average T-S-C was obtained as listed in equation 3. The crack opening (ω) is transformed into the strain (ϵ) by dividing it by the crack spacing [Massicotte, 2003].

5.2 Static Test of SFRC Beam

One beam of series two (SLB-1) was tested under a four-point loading flexure test monotonically achieving a flexural capacity of 28.875-kN.m, Figure 6 shows the beam at failure. The load versus deflection curve under static load is given in Figure 7. The rebar strain, concrete strain, and N.A. position were recorded in the constant moment region until a tensile ductile failure of steel rebars followed by concrete crushing in the compression zone. The average of experimental values was compared with those calculated from the section analysis during the load test. Best fitting was achieved between experimental and calculated results with less error, as shown



(a) Left side cracks.



(b) Right side cracks.

Figure 6: Failure of SFRC beam under static test.

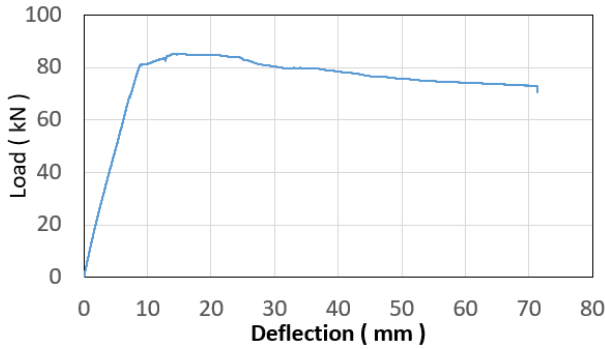


Figure 7: Load versus deflection of the SFRC beam under static test.

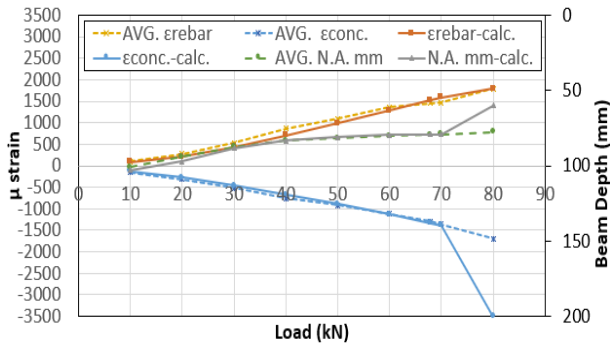
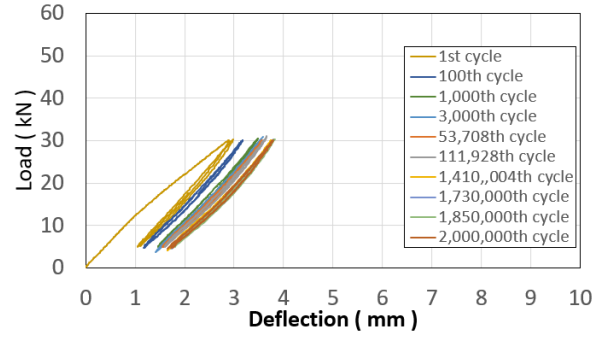


Figure 8: Experimental versus calculated results of SFRC beam under static test.

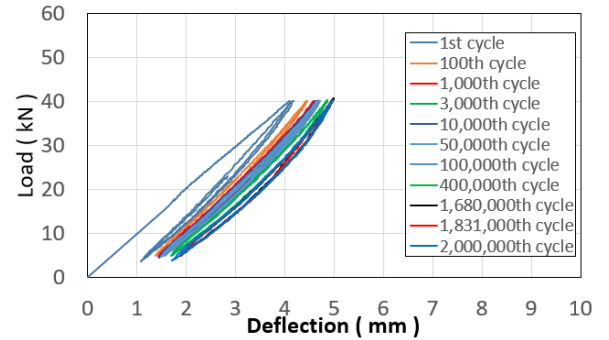
in Figure 8, that the left axis shows the rebar and concrete strain, and right axis shows the N.A. position through the SFRC beam's depth.

5.3 Fatigue Test of SFRC Beams

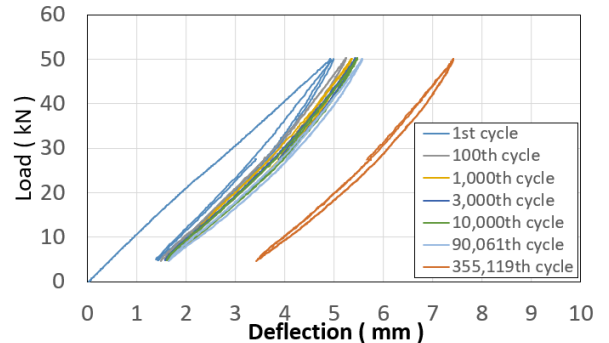
Three beams of series two (FLB-30, FLB-



(a) FLB-30



(b) FLB-40



(c) FLB-50

Figure 9: Load versus deflection of SFRC beams during the fatigue test.

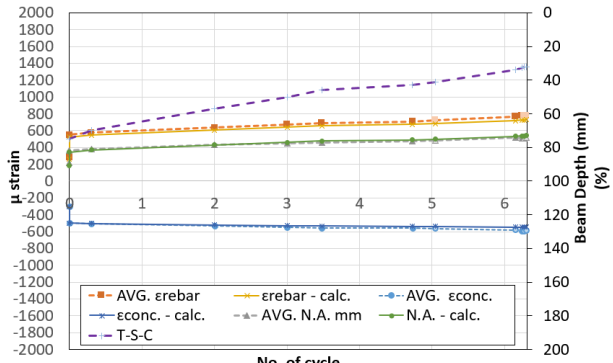
40, and FLB-50) were tested under a four-point loading flexure fatigue test. The load versus deflection curves under fatigue load during fatigue life of three beams are given in Figure 9.

All three beams (FLB-30, FLB-40, and FLB-50) were under fatigue sinusoidal loads with min load of 5.0-kN and a different max load of 30-kN, 40-kN, 50-kN respectively.

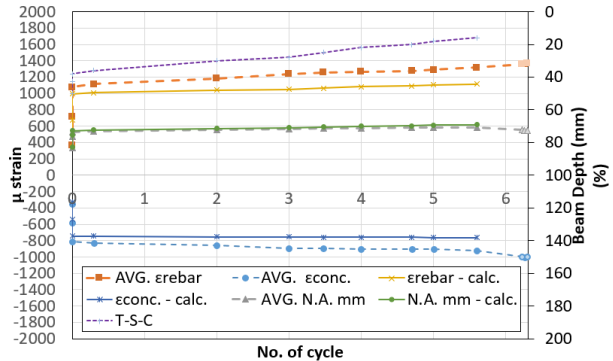
The rebar strain, concrete strain, and N.A. position were also recorded in the constant moment region until the end of two million cycles for FLB-30 and FLB-40 or fatigue rebar brittle failure for FLB-50 at 380,116 cycles. The average of experimental values was also

compared with those calculated from the section analysis calculation method by assuming a loss of the bridging strength carried by fibers during the fatigue life.

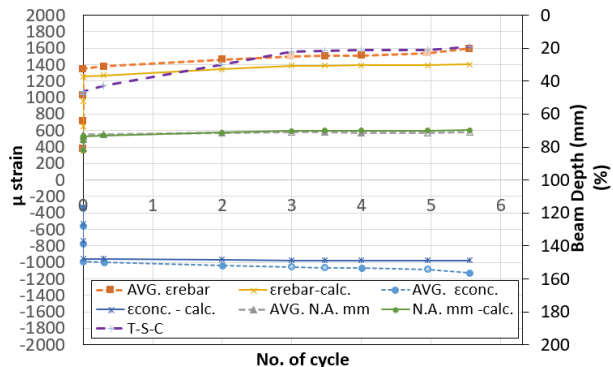
It is acceptable to observe the same tendency from both experiment and section calculation results with a minimum error by using a degraded T-S-C, even though at the first cycle, because the cracks initiated at the weakest plane, that may have fewer fibers dosage or different fibers orientation which may give less fracture energy than that was delivered from average notched beam results in section 5.1.



(a) FLB-30



(b) FLB-40



(c) FLB-50

Figure 10: Experimental versus calculated results of SFRC beam during the fatigue test.

Figure 10 shows the section analysis calculations regarding the experimental results. In case of low-stress levels such as beams FLB-30 and FLB-40, the degradation in the bridging strength follows a linear proportion during the fatigue life until the end of two million cycles, as shown by the purple broken lines that showing the used amount of fracture energy of original T-S-C indicated in the right axis as a percentage. On the other hand, in case of high stress level as FLB-50 the degradation in the bridging strength follows a linear proportion until certain fatigue life, nearly 1,000-cycles, after that the beam sustain with a certain amount of bridging strength until a rupture failure of steel rebar happened suddenly, as observed by the almost horizontal purple broken line.

6 CONCLUSIONS

The behavior of SFRC beams reinforced with conventional rebars subjected to fatigue loading has been investigated. The experimental results for SFRC beams and the results from the section analysis calculation method were compared by assuming losing in the bridging strength carried by fibers during the fatigue life. The results are summarized as follows:

1. The static flexural behavior of SFRC beams with conventional rebars can be evaluated by using the T-S-C obtained from the material level test.
2. The fatigue flexural behavior of SFRC beams with conventional rebars under low-stress level can be assessed by assuming an incremental degradation of the bridging strength during fatigue life.
3. For a high level of fatigue stress, the flexural behavior of SFRC beams can be estimated as low-stress level until a limited degree of bridging strength, prior brittle failure of rebar when a higher increase in the deflection takes place.

Finally, it is concluded that by assuming a degradation level of T-S-C obtained from

material level in the section analysis calculations, a full design approach for SFRC beams under flexural fatigue load is supposed to be developed.

REFERENCES

- [1] Mallet, G.P., 1991. "Fatigue of reinforced concrete", Her Majesty's Stationery Office, London.
- [2] CEB, 1988. "Fatigue of concrete structures, state of the art report", CE.
- [3] Tejchman, J., and Kozicki, J., 2010. "Experimental and theoretical investigations of steel fibrous concrete", Springer, Berlin.
- [4] Lee, M. K. and Barr, B. I. G., 2004. "An overview of the fatigue behavior of plain and fibre reinforced concrete", *Cement and Concrete Composites*, 26(4): 299-305.
- [5] Parvez A, Foster SJ., 2015. "Fatigue behavior of steel-fibre-reinforced concrete beams.", *Struct Eng*,141(4).
- [6] RILEM-Committee-TDF-162, Chairlady L. Vandewalle, 2003. "Test and Design Methods for Steel fiber Reinforced Concrete. Design of Steel Fibre Reinforced Concrete using the σ -w Method: Principles and Applications", *Mat.Struc*.
- [7] Japan Concrete Institute (JCI), 2003. "Method of Test for Fracture Energy of Concrete by Use of Notched Beams.", JCI.
- [8] Massicotte B., Barros J., Rossi P., 2003. "Design of SFRC members in flexure: application to a building floor, Dimensionato de estruturas de betão reforçado com fibras de aço", *DEC-UM, Portugal*, (4):1-17.